J. Fluid Mech. (1974), *vol.* 65, *part* 3, *pp.* 461–480
Printed in Great Britain

Symmetrical flow past a uniformly accelerated circular cylinder

By W. M. COLLINS AND S. C. R. DENNIS

Department of Applied Mathematics, University of Western Ontario, London, Canada

(Received 15 August 1973)

The flow normal to an infinite circular cylinder which is uniformly accelerated from rest in a viscous fluid is considered. The flow is assumed to remain symmetrical about the direction of motion of the cylinder. Two types of solution are presented. In the first an expansion in powers of the time from the start of the motion is given which extends the results of boundary-layer theory by taking into account corrections for finite Reynolds numbers. Physical properties of the flow for small times and finite but large Reynolds numbers are calculated from this expansion. In the second method of solution the Navier–Stokes equations are integrated by an accurate procedure which is a logical extension of the solution in powers of the time. Results are obtained for $R^2 = 97{\cdot}5$, 5850, 122×10^3 and ∞, where R is the Reynolds number. This is defined as $R = 2a(ab)^{\frac{1}{2}}/\nu$, where a is the radius of the cylinder, b the uniform acceleration and ν the kinematic viscosity of the fluid. The methods are in good agreement for small times.

The numerical method of integration has been carried to moderate times and various flow properties have been calculated. The growth of the length of the separated wake behind the cylinder for $R^2 = 97{\cdot}5$, 5850 and 122×10^3 is compared with the results of recent experimental measurements. The agreement is only moderate for $R^2 = 97{\cdot}5$ but it improves greatly as R increases. The numerical integrations were continued in each case until the implicit method of integration failed to converge, which terminated the procedure. A secondary vortex appeared on the surface of the cylinder for the case $R^2 = 122 \times 10^3$.

1. Introduction

The initial motion of a viscous incompressible fluid normal to a cylinder of infinite length and arbitrary cross-section has previously been treated using unsteady boundary-layer theory. Blasius (1908) considered the general problem for two cases of motion from rest. In the first the body is started impulsively and then moves with constant velocity, and in the second it is accelerated uniformly. Two approximations to the initial flow were obtained in the first case and three in the second. A third approximation was subsequently given for the impulsively started case by Goldstein & Rosenhead (1936). The theory has been generalized to other types of variation of the initial velocity of the cylinder by Görtler (1944, 1948) and by Watson (1955). In all cases the method of procedure was to obtain successive approximations which form a series in

powers of the time from the start of the motion. The leading term is valid for all values of the Reynolds number R, but subsequent terms in the expansion are valid only in the case $R \to \infty$.

Recent work by Wang (1967) and Collins & Dennis (1973*a*) has extended the theory for an impulsively started circular cylinder to finite values of R by determining corrections of second and higher orders valid for large R. These extensions are based on the full Navier–Stokes equations rather than the boundary-layer equations. All the series expansions are, however, limited in validity to small times. Collins & Dennis (1973*b*) made a numerical extension of the method of expansion in powers of the time for an impulsively started circular cylinder by using an implicit time-dependent numerical integration procedure. In this way accurate numerical solutions of the Navier–Stokes equations were obtained up to quite moderate times over a wide range of Reynolds numbers. The calculated results were found to agree well with previous numerical and experimental work.

In the present paper the methods of expansion in powers of the time and numerical integration are both applied to the case of the uniformly accelerated start, the second of the cases treated in detail by Blasius (1908). Higher-order corrections to boundary-layer theory do not appear previously to have been considered for this problem and neither does the question of extending the boundary-layer results beyond the first three terms of the expansion in powers of the time previously given by Blasius (1908). There also do not appear to be any previous numerical solutions of the Navier–Stokes equations in this case. Numerical work on this problem is of current interest in view of the recent experiments described by Taneda (1972). In these experiments the time of separation of the flow and the subsequent growth of the separated wake have been measured over a range of Reynolds numbers. Other properties of the flow, such as the appearance of secondary vortices at high Reynolds numbers, were also observed. Separated flows of this nature are of fundamental importance and the present calculations provide the opportunity of giving theoretical confirmation of these observations.

Detailed numerical calculations are given for the cases $R^2 = 97{\cdot}5$, 5850 and 122×10^3 and also for the boundary-layer case $R = \infty$. The finite values of R correspond to three cases considered experimentally by Taneda (1972). The numerical integrations are independent of the expansions in powers of the time and are carried out to times well beyond the range of validity of these expansions. It is therefore possible to use the numerical integrations to check the series expansions at small times. The results for $R = \infty$ are found to verify the extensions of the boundary-layer results of Blasius (1908) given by the series expansion and the results for finite Reynolds numbers check well with the corrections of second and higher orders.

2. Basic equations

Modified polar co-ordinates (ξ, θ) are used, where $\xi = \log(r/a)$ and a is the radius of the cylinder, with the centre of the cylinder as origin. At time $t = 0$ the cylinder starts to move in the direction $\theta = \pi$ with uniform acceleration b.

If ψ' and ζ' are the stream function and vorticity associated with the motion, we introduce the dimensionless functions ψ and ζ defined by the equations

$$\psi' = a(ab)^{\frac{1}{2}}\psi, \quad \zeta' = -(b/a)^{\frac{1}{2}}\zeta.$$

Dimensionless radial and transverse components of velocity (u, v) are obtained by dividing the corresponding dimensional components by $(ab)^{\frac{1}{2}}$. We then have

$$u = e^{-\xi}\partial\psi/\partial\theta, \quad v = -e^{-\xi}\partial\psi/\partial\xi \tag{1}$$

and

$$\zeta = e^{-\xi}\left(\frac{\partial u}{\partial\theta} - \frac{\partial v}{\partial\xi} - v\right), \tag{2}$$

where ψ and ζ satisfy the equations

$$\partial^2\psi/\partial\xi^2 + \partial^2\psi/\partial\theta^2 = e^{2\xi}\zeta \tag{3}$$

and

$$e^{2\xi}\frac{\partial\zeta}{\partial\tau} = \frac{2}{R}\left(\frac{\partial^2\zeta}{\partial\xi^2} + \frac{\partial^2\zeta}{\partial\theta^2}\right) - \frac{\partial\psi}{\partial\theta}\frac{\partial\zeta}{\partial\xi} + \frac{\partial\psi}{\partial\xi}\frac{\partial\zeta}{\partial\theta}. \tag{4}$$

Here $\tau = (b/a)^{\frac{1}{2}}t$, $R = 2a(ab)^{\frac{1}{2}}/\nu$, and ν is the coefficient of kinematic viscosity. The boundary conditions for $\tau > 0$ are that

$$\psi = \partial\psi/\partial\xi = 0 \quad \text{when} \quad \xi = 0 \tag{5}$$

and

$$e^{-\xi}\partial\psi/\partial\xi \to \tau\sin\theta, \quad e^{-\xi}\partial\psi/\partial\theta \to \tau\cos\theta \quad \text{as} \quad \xi \to \infty. \tag{6}$$

The last conditions correspond to a uniformly accelerated stream relative to the cylinder at large distances from it.

The flow is assumed to remain symmetrical about the direction of motion. We may therefore assume the expansions

$$\psi = \sum_{n=1}^{\infty} f_n(\xi, \tau)\sin n\theta, \quad \zeta = \sum_{n=1}^{\infty} g_n(\xi, \tau)\sin n\theta. \tag{7), (8}$$

This is the same form of solution as that adopted by Collins & Dennis (1973*a*, *b*) and it is also generally consistent with the principle of the spectral methods recently discussed by Orszag (1970, 1971). If the expressions (7) and (8) are substituted in (3) and (4), sets of differential equations for the functions $f_n(\xi, \tau)$ and $g_n(\xi, \tau)$ are obtained. These sets of equations can be written as

$$\partial^2 f_n/\partial\xi^2 - n^2 f_n = e^{2\xi}g_n \tag{9}$$

and

$$e^{2\xi}\frac{\partial g_n}{\partial\tau} = \frac{2}{R}\frac{\partial^2 g_n}{\partial\xi^2} + nf_{2n}\frac{\partial g_n}{\partial\xi} + \left(\tfrac{1}{2}n\frac{\partial f_{2n}}{\partial\xi} - \frac{2}{R}n^2\right)g_n + S_n, \tag{10}$$

where

$$S_n = \frac{1}{2}\sum_{\substack{m=1 \\ m\neq n}}^{\infty}\left\{[(m+n)f_{m+n} - jf_j]\frac{\partial g_m}{\partial\xi} + m\left[\frac{\partial f_{m+n}}{\partial\xi} - \operatorname{sgn}(m-n)\frac{\partial f_j}{\partial\xi}\right]g_m\right\}. \tag{11}$$

Here $j = |m-n|$ and $\operatorname{sgn}(m-n)$ is equal to $+1$ if $m > n$, -1 if $m < n$ and zero if $m = n$.

The two sets of equations (9) and (10) hold for all positive integer values of n. They are the same equations as those which form the basis of the numerical integrations of Collins & Dennis (1973*b*). In the present paper they are also

used to generate the series in powers of τ, so that all the details of the present work are contained in (9) and (10) and the boundary conditions. The latter are that

$$f_n = \partial f_n/\partial\xi = 0 \quad \text{when} \quad \xi = 0, \tag{12}$$

which follow from (5), and

$$e^{-\xi} f_n \to \tau\delta_n, \quad e^{-\xi}\,\partial f_n/\partial\xi \to \tau\delta_n \quad \text{as} \quad \xi \to \infty, \tag{13}$$

which follow from (6), where $\delta_1 = 1$ and $\delta_n = 0\,(n \neq 1)$. A further condition which follows from (6) is that $\zeta \to 0$ as $\xi \to \infty$, and hence each $g_n(\xi, \tau)$ in (8) must satisfy the condition

$$g_n(\xi, \tau) \to 0 \quad \text{as} \quad \xi \to \infty. \tag{14}$$

Finally, on multiplying (9) by $e^{-n\xi}$ and integrating from $\xi = 0$ to $\xi = \infty$, making use of both of (12) and (13), the condition

$$\int_0^\infty e^{(2-n)\xi} g_n(\xi, \tau)\, d\xi = 2\tau\delta_n \tag{15}$$

may be deduced. This condition is used to replace (13), and the set of conditions (12), (14) and (15) is sufficient to solve the problem. It may be shown, following Collins & Dennis (1973*a*), that, provided that these three latter conditions are satisfied and that $e^{2\xi} g_n(\xi, \tau)$ is bounded as $\xi \to \infty$ for all n at any value of τ, then the conditions (13) are automatically satisfied.

In the initial boundary layer formed during a uniformly accelerated start it is known (Blasius 1908) that the boundary-layer thickness is proportional to $k = 2(2\tau/R)^{\frac{1}{2}}$ and that ψ and ζ are proportional to τk and τk^{-1} respectively In order to deal with the initial flow we therefore make the transformations

$$\xi = kx, \quad f_n = k\tau F_n, \quad g_n = \tau G_n/k \tag{16}$$

in the sets of equations (9) and (10). The first set becomes

$$\partial^2 F_n/\partial x^2 - n^2 k^2 F_n = e^{2kx} G_n \tag{17}$$

and the second yields

$$4\tau \frac{\partial G_n}{\partial \tau} = e^{-2kx} \frac{\partial^2 G_n}{\partial x^2} + (2x + 4n\tau^2 F_{2n}\, e^{-2kx}) \frac{\partial G_n}{\partial x} - \left[2 + e^{-2kx}\left(n^2k^2 - 2n\tau^2 \frac{\partial F_{2n}}{\partial x}\right)\right] G_n + 4\tau^2 e^{-2kx} S_n^*, \tag{18}$$

where S_n^* is S_n with f_n replaced by F_n, g_n replaced by G_n and ξ replaced by x. The boundary conditions become

$$F_n = \partial F_n/\partial x = 0 \quad \text{when} \quad x = 0, \tag{19}$$

$$G_n(x, \tau) \to 0 \quad \text{as} \quad x \to \infty \tag{20}$$

and

$$\int_0^\infty e^{(2-n)\,kx} G_n(x, \tau)\, dx = 2\delta_n. \tag{21}$$

The initial solution is found by putting $\tau = 0$ (and hence $k = 0$) in (17) and (18) and in the condition (21). The set of equations (18) becomes

$$\frac{\partial^2 G_n}{\partial x^2} + 2x\frac{\partial G_n}{\partial x} - 2G_n = 0. \tag{22}$$

The only solutions which satisfy the conditions (20) and (21) are

$$G_1(x, 0) = -8[x(1 - \operatorname{erf} x) - \pi^{-\frac{1}{2}} e^{-x^2}], \quad G_n(x, 0) = 0 \quad (n = 2, 3, \ldots). \tag{23}$$

The corresponding initial solutions of (17) subject to the conditions (19) are

$$\left.\begin{aligned} F_1(x, 0) &= \tfrac{4}{3}[x^3(\operatorname{erf} x - 1) + \tfrac{3}{2}x \operatorname{erf} x + \pi^{-\frac{1}{2}}\{(x^2 + 1)\, e^{-x^2} - 1\}], \\ F_n(x, 0) &= 0 \quad (n = 2, 3, \ldots). \end{aligned}\right\} \tag{24}$$

The expressions (23) and (24) are consistent with the first approximation to the solution of the boundary-layer equations given by Blasius (1908) for the uniformly accelerated case. The expressions are valid for any Reynolds number at the start of the motion, although only for very small times, particularly for low R.

The first approximation to the stream function obtained from (24) gives rise to an initial approximation to the dimensionless transverse velocity component given by

$$v = \tau[-2 \operatorname{erf} x + 4x^2(1 - \operatorname{erf} x) - 4\pi^{-\frac{1}{2}} x\, e^{-x^2}] \sin\theta. \tag{25}$$

This is consistent as $x \to \infty$ with the transverse velocity component of the corresponding potential flow evaluated at the cylinder surface. The initial approximation to the radial velocity component corresponding to (24) is of order k in the boundary layer but is not consistent as $x \to \infty$ with the radial velocity component of the corresponding potential flow at the cylinder surface. An approximation to the initial stream function which rectifies this situation and which tends to a uniformly accelerated stream as $\xi \to \infty$ can be found by obtaining the solution of (22) which satisfies (20), adjusting the constant of integration to satisfy the full equation (21) with $k \neq 0$, and finally substituting in the full equation (17), again with $k \neq 0$, and integrating subject to (19). The procedure is similar to that already given by Collins & Dennis (1973*a*, p. 60).

In the present paper the set of equations (23) is used to give initial conditions for the numerical solution of the sets of equations (17) and (18) subject to the conditions (19)–(21). The method of solution is that given by Collins & Dennis (1973*b*) and will be referred to briefly later. It is also possible to obtain further approximations to the flow, valid for small τ and large R, from (17) and (18). These are of some theoretical interest but they also have practical value in that they may be used to check the numerical procedure at small values of τ. These approximations will now be described, but only briefly since they can also be developed by direct extension of the methods given by Collins & Dennis (1973*a*).

3. Expansion in powers of k and τ

If R is large and τ small then k is small and it is found to be possible to expand the functions $F_n(x, \tau)$ and $G_n(x, \tau)$ which satisfy (17) and (18) as power series in k. It is then found that the functional coefficient of each power of k can itself be

expanded as a power series in τ in which only even powers of τ occur. This is consistent with the successive approximations obtained by Blasius (1908) in the method of solution given for the boundary-layer equations ($k = 0$) in the case of a uniformly accelerated cylinder. In the present paper the same structure is found to hold for higher powers of k. We may therefore write

$$F_n(x,\tau) = \sum_{i=0}^{\infty} \sum_{j=0}^{\infty} F_n^{(i,j)}(x)\, k^i \tau^{2j}, \tag{26}$$

$$G_n(x,\tau) = \sum_{i=0}^{\infty} \sum_{j=0}^{\infty} G_n^{(i,j)}(x)\, k^i \tau^{2j}. \tag{27}$$

These are substituted in (17) and (18) and the exponentials which occur are expanded in powers of k. If the coefficients of each term $k^i\tau^{2j}$ are equated to zero, sets of equations for the functions $F_n^{(i,j)}(x)$ and $G_n^{(i,j)}(x)$ are obtained. These are quite complicated in general and will not be given in detail.

Boundary conditions follow from (19)–(21). The functions $F_n^{(i,j)}(x)$ must obviously individually satisfy (19) and the functions $G_n^{(i,j)}(x)$ must satisfy (20). A set of conditions corresponding to (21) may be obtained by substituting (27) in the integral, expanding the exponential in powers of k and then equating the coefficients of each term $k^i\tau^{2j}$ on either side of the equation. The general form of these conditions will again not be given, but it may be noted that the only inhomogeneous condition for the functions $G_n^{(i,j)}(x)$ which arises is for the case $i = 0, j = 0, n = 1$ and that the function $G_1^{(0,0)}(x)$ which satisfies it is the function $G_1(x,0)$ given in (23). Brief details of the procedure for obtaining solutions will now be given, together with a few exact solutions obtained. In describing the procedure it is convenient to suppress the superscripts and denote $G_n^{(i,j)}(x)$ simply by $G_n(x)$.

On substitution of (26) and (27) in (18), it is found that the function $G_n^{(i,j)}(x)$ satisfies an equation of the form

$$G_n'' + 2xG_n' - 2(i + 4j + 1)\, G_n = r_n(x), \tag{28}$$

where a prime denotes differentiation with regard to x. The problem of generating solutions of (28) for given i, j and n is always one of successive approximation. Thus for fixed i, solutions for all appropriate n can be obtained successively for increasing j, since $r_n(x)$ depends only on previously determined functions and is thus known completely at each value of j. We require $G_n(x)$ to vanish as $x \to \infty$ and an appropriate solution of (28) is

$$G_n(x) = A_n e^{-\frac{1}{2}x^2} D_\lambda(2^{\frac{1}{2}}x) + G_n^*(x), \tag{29}$$

where $G_n^*(x)$ is any particular solution of (28) which vanishes as $x \to \infty$. Here D_λ is the parabolic cylinder function with $\lambda = -2 - i - 4j$, and A_n is a constant to be determined. Once $G_n^*(x)$ has been determined, A_n is found by substituting (29) into the appropriate condition deduced from (21) and performing the necessary integrations. Finally, the corresponding function $F_n^{(i,j)}(x)$ in the expansion (26) is found by substituting (29) into a second-order differential equation deduced from (17) and integrating twice subject to (19).

Exact solutions can be obtained for a few of the functions $G_n^*(x)$, but exact analysis cannot be carried very far. First, the functions $r_n(x)$ rapidly become complicated as i and j increase. The problem of finding $G_n^*(x)$ is then very tedious. A second reason is that, whereas for small j all but the first few $r_n(x)$ are identically zero, which makes $G_n^*(x)$ zero also, as j increases the number of non-zero $r_n(x)$ also increases and there are more $G_n^*(x)$ to be found. It is much easier to continue the process by numerical methods by computing each $r_n(x)$ and $G_n^*(x)$ numerically. The procedure used to determine numerical solutions of (28) which satisfy the required conditions is virtually identical to that described by Collins & Dennis (1973*a*, p. 67). The same grid size 0·05 was used, and also the same value $x = 6$ at which the approximation to the condition at infinity was assumed.

4. Detailed terms in the expansion

Terms in the series (26) and (27) up to and including the terms in k^3 have been calculated, mostly by numerical methods. For $i = 0$ (the boundary-layer case) the terms have been calculated up to $j = 7$, for $i = 1$ up to $j = 6$, for $i = 2$ up to $j = 5$ and for $i = 3$ up to $j = 4$, in all cases inclusive. The details are now given for each power of k.

(*a*) $i = 0$. The solution for $j = 0$ is given by (23) and (24). For $j \neq 0$ the condition on the function $G_n^{(i,j)}(x)$ which corresponds to (21) is

$$\int_0^\infty G_n^{(0,j)}(x)\,dx = 0. \tag{30}$$

For $j = 1$ the equations of type (28) derived from (18) have $r_n(x) \equiv 0$ for all n except $n = 2$. In this case

$$\begin{aligned} r_2(x) = \tfrac{32}{3}[&4x^3 \operatorname{erf} x(2 - \operatorname{erf} x) - 4x^3 + 2\pi^{-\frac{1}{2}}(1 - \operatorname{erf} x) \\ &- \pi^{-\frac{1}{2}}(10x^2 + 1)\,e^{-x^2} \operatorname{erf} x + 2\pi^{-\frac{1}{2}}(5x^2 - 1)\,e^{-x^2} - 6\pi^{-1}x\,e^{-2x^2}]. \end{aligned} \tag{31}$$

We then find

$$\begin{aligned} G_2^{(0,1)}(x) = {}& (4x^5 + 20x^3 + 15x)(A + B \operatorname{erf} x) - \tfrac{2}{3}x(4x^4 + 4x^2 + 3)(\operatorname{erf} x)^2 \\ &- (\tfrac{64}{3}x^3 + 16x - \tfrac{32}{15}\pi^{-\frac{1}{2}}) \operatorname{erf} x - \tfrac{2}{3}\pi^{-\frac{1}{2}}(8x^4 + 2x^2 + 1)\,e^{-x^2} \operatorname{erf} x \\ &+ \pi^{-\frac{1}{2}}[4Bx^4 + (18B - \tfrac{68}{3})x^2 + (8B - \tfrac{22}{3})]\,e^{-x^2} \\ &+ \tfrac{32}{3}x^3 + 8x - \tfrac{32}{15}\pi^{-\frac{1}{2}} - \tfrac{4}{3}\pi^{-1}x(2x^2 - 1)\,e^{-2x^2}, \end{aligned} \tag{32}$$

where $A = -64/225\pi$ and $B = \frac{2}{3} + 64/225\pi$. The general form of the equations (17) and the conditions (19) for the functions $F_n^{(0,j)}(x)$ are respectively

$$F_n'' = G_n, \quad F_n(0) = F_n'(0) = 0 \tag{33a, b}$$

and hence the corresponding function $F_2^{(0,1)}(x)$ is obtained by integrating (33*a*) twice subject to the initial conditions. The precise expression will not be given.

For $j = 2, \ldots, 7$ the solutions of (28) and corresponding solutions of (33) have been obtained using numerical methods. Each solution of (28) must vanish as $x \to \infty$ and satisfy (30). The values of n associated with each j for which $r_n(x)$ is not identically zero are $n = 1, 3$ for $j = 2$, $n = 2, 4$ for $j = 3$, $n = 1, 3, 5$ for $j = 4$, $n = 2, 4, 6$ for $j = 5$, $n = 1, 3, 5, 7$ for $j = 6$ and $n = 2, 4, 6, 8$ for $j = 7$.

These give the only non-zero terms in the expansions (26) and (27) as far as the term in τ^{14} for the case $i = 0$.

(*b*) $i = 1$. This corresponds to the first-order correction to boundary-layer theory. In this case the condition deduced from (21) is

$$\int_0^\infty \{G_n^{(1,j)}(x) + (2-n)\,xG_n^{(0,j)}(x)\}\,dx = 0. \tag{34}$$

For $j = 0$ the only $r_n(x)$ in (28) which is not identically zero is that for $n = 1$, given by

$$r_1(x) = 32\pi^{-\frac{1}{2}}x\,e^{-x^2}. \tag{35}$$

From this we obtain

$$G_1^{(1,0)}(x) = (2x^2+1)\,(1-\operatorname{erf}x) - 6\pi^{-\frac{1}{2}}x\,e^{-x^2}. \tag{36}$$

The equation and initial conditions for the functions $F_n^{(1,j)}(x)$ are respectively

$$F_n'' = G_n^{(1,j)} + 2xG_n^{(0,j)}, \quad F_n(0) = F_n'(0) = 0. \tag{37}$$

From these we obtain

$$F_1^{(1,0)}(x) = \tfrac{7}{6}x^4(\operatorname{erf}x - 1) + \tfrac{1}{12}\pi^{-\frac{1}{2}}(14x^3 - 13x)\,e^{-x^2} + \tfrac{4}{3}\pi^{-\frac{1}{2}}x + \tfrac{1}{2}x^2(1-\operatorname{erf}x) - \tfrac{1}{8}\operatorname{erf}x. \tag{38}$$

It becomes too complicated to obtain further terms by exact analysis, but terms with $j = 1$ up to $j = 6$ have been tabulated using numerical methods. The values of n associated with each value of j for which the $r_n(x)$ in (28) are not identically zero are exactly the same as for the case $i = 0$, and a similar situation exists for the cases $i = 2$ and 3 to follow.

(*c*) $i = 2$. There is hardly any need to give further equations and conditions satisfied by these functions, except that it may be noted that this case is the first one in which the terms $\partial^2\psi/\partial\theta^2$ in (3) and $\partial^2\zeta/\partial\theta^2$ in (4) start to exert an influence. An exact solution has been found for the term with $j = 0$ in which the only non-zero $r_n(x)$ in (28) is

$$r_1(x) = -8\pi^{-\frac{1}{2}}(4x^4 - 2x^2 - 1)\,e^{-x^2}. \tag{39}$$

This leads to the expressions

$$G_1^{(2,0)}(x) = x(\tfrac{2}{3}x^2+1)\,(\operatorname{erf}x - 1) + \tfrac{1}{6}\pi^{-\frac{1}{2}}(12x^4 + 8x^2 - 1)\,e^{-x^2} \tag{40}$$

and

$$F_1^{(2,0)}(x) = \tfrac{7}{10}x^5(\operatorname{erf}x - 1) + \tfrac{1}{6}x^3(\operatorname{erf}x + 1) + \tfrac{1}{8}x\operatorname{erf}x + \tfrac{1}{60}\pi^{-\frac{1}{2}} \times (42x^4 + 19x^2 - 1)\,e^{-x^2} - \tfrac{2}{3}\pi^{-\frac{1}{2}}x^2 + \tfrac{1}{60}\pi^{-\frac{1}{2}}. \tag{41}$$

Numerical solutions have been obtained for the terms with $j = 1$ up to $j = 5$.

(*d*) $i = 3$. An exact solution has been obtained for $j = 0$. The non-zero $r_n(x)$ in (28) is

$$r_1(x) = (2x^2+1)\,(1-\operatorname{erf}x) + \tfrac{4}{3}\pi^{-\frac{1}{2}}(12x^7 - 26x^5 + x^3 - 6x)\,e^{-x^2}. \tag{42}$$

This leads to the expressions

$$G_1^{(3,0)}(x) = \tfrac{1}{32}(12x^4 + 20x^2 + 1)\,(1-\operatorname{erf}x) - \tfrac{1}{48}\pi^{-\frac{1}{2}} \times (32x^7 - 16x^5 + 2x^3 - 11x)\,e^{-x^2} \tag{43}$$

and

$$F_1^{(3,0)}(x) = \tfrac{1}{1440}(422x^6 - 45x^4)(\operatorname{erf} x - 1) + \tfrac{1}{64}x^2(1 - 5\operatorname{erf} x) + \pi^{-\frac{1}{2}}x \times (\tfrac{2}{9}x^2 - \tfrac{1}{60}) + \tfrac{235}{384}\operatorname{erf} x + \tfrac{1}{2880}\pi^{-\frac{1}{2}}(3629x^5 - 212x^3 - 3477x)\, e^{-x^2}. \quad (44)$$

Numerical solutions have been obtained for all non-zero terms corresponding to $j = 1$ up to $j = 4$. One advantage of obtaining at least one exact solution for each value of i is that it gives at least some check on the numerical procedure. The exact solutions were checked numerically and the comparison was found to be satisfactory.

5. Numerical integration procedure

The expansions in powers of k and τ enable properties of the flow to be calculated for large R and small τ, although nothing precise can be said about the region of convergence of the series. In order to calculate the flow for any Reynolds number and large enough time, in particular for some of the experimental studies described by Taneda (1972), the numerical method of integration given by Collins & Dennis (1973*b*) may be used. The solution is started by integrating (17) and (18) using (23) as an initial condition and (19)–(21) as boundary conditions. Then, at some later value of τ after the boundary layer has thickened, the integration is switched to (9) and (10) and continued subject to the conditions (12), (14) and (15) in the natural space co-ordinate ξ. An implicit method of integration of Crank–Nicolson type is used, and a given approximation to the flow is obtained by truncating the series (7) and (8). This is done by setting to zero all functions $f_n(\xi, \tau)$ and $g_n(\xi, \tau)$ for $n > n_0$, where n_0 is an integer defining the order of the truncation. Thus in practice $2n_0$ functions are determined from (9) and (10) [or (17) and (18)].

The essential details of the procedure have been described by Collins & Dennis (1973*b*). As in the case of the impulsive start, only a few functions $F_n(x, \tau)$ and $G_n(x, \tau)$ are needed to describe the motion for small τ in view of the initial structure given by (23) and (24). More functions are added as the integration proceeds and the parameter n_0 actually refers to the maximum number of terms used in each of the series (7) and (8) during the integration. It is also necessary to use a small time step for small τ. The reason is the same as in the impulsively started case. The series expansions of $F_n(x, \tau)$ and $G_n(x, \tau)$ involve odd powers of k and hence all derivatives with respect to τ after some stage are singular at $\tau = 0$. The problem does not arise in the boundary-layer case, where $k = 0$. For the cases of finite R considered the integrations were all started by taking 10 time steps $H = 10^{-4}$ followed by 24 steps $H = 10^{-3}$, bringing the integrations to $\tau = 0{\cdot}025$. The integration was then continued using a step $H = 0{\cdot}0125$. The grid size in the x co-ordinate was taken as $h_x = 0{\cdot}05$ in all cases. The maximum value of x in the field (at which the condition $G_n(x, \tau) = 0$ is assumed) was taken as $x = 8$.

The integration is switched from (17) and (18) to (9) and (10) at some time $\tau = \tau_0$. The choice of τ_0 is empirical, but since the same grid points in both the x and ξ co-ordinates must be used, the grid size h in the ξ co-ordinate must be such that $h = 2(2\tau_0/R)^{\frac{1}{2}} h_x$. In fact τ_0 is merely chosen so that h is reasonably

R^2	τ_M	τ_0	h	ξ_M	n_0
97·5	9·8	0·7875	0·0400	6·39	20
5850	4·7	4·0375	0·0325	5·20	20
122×10^3	3·2	—	—	—	20
∞	1·6	—	—	—	20

TABLE 1. Parameters used in the numerical solutions

small. The integration is then continued in the co-ordinates ξ and τ until some final time $\tau = \tau_M$ is reached. Integrations were carried out for the three finite values of R given by $R^2 = 97{\cdot}5$, 5850 and 122×10^3 and $R = \infty$. In each case the value τ_M was determined by the fact that the implicit method of integration failed to converge. Failure at $\tau = \tau_M$ does not invalidate the results for $\tau < \tau_M$ in view of the step-by-step nature of the calculation. The accuracy criterion for convergence for all $\tau < \tau_M$ was the same as that given by Collins & Dennis (1973*b*, p. 112).

Values of the various parameters used in the calculations are shown in table 1. The value of the field length is denoted by $\xi = \xi_M$. This is the value where the condition $g_n(\xi, \tau) = 0$ is assumed. The parameter n_0 is the maximum number of terms in (7) and (8) employed during the integration, which is actually the number employed at the final time $\tau = \tau_M$. In the case $R^2 = 122 \times 10^3$ the integration was terminated while still in the boundary-layer co-ordinates.

6. Results

We shall first give results obtained from the series expansions in powers of k and τ, followed by results obtained from the purely numerical method. For the case $R = \infty$, Blasius (1908) obtained two approximations to the time of separation. Separation first occurs at the rear generator. It occurs at a time $\tau = T$, say, defined by the condition $\partial\zeta/\partial\theta = 0$, when $x = 0$ and $\theta = 0$. From the expansion (27) in powers of k and τ we can obtain various approximations to T by investigating the roots of the equation

$$\sum_{n=1}^{n_1} \sum_{i=0}^{i_1} \sum_{j=0}^{j_1} n k^i T^{2j} G_n^{(i,j)}(0) = 0. \tag{45}$$

Here i_1 and j_1 correspond to the total number of terms taken in (27) and the sum over n corresponds to all the non-zero terms $G_n^{(i,j)}(x)$ associated with each value of i and j. The boundary-layer case corresponds to $i_1 = 0$ and successive approximations to T are obtained by taking increasing values of j_1.

If we take $j_1 = 1$ in the boundary-layer case we obtain

$$T^2 = 450\pi/(465\pi - 256) = 1{\cdot}173,$$

which is in agreement with the first approximation given by Blasius (1908). The second approximation ($j_1 = 2$) gives T^2 as the positive root of the equation

$$0{\cdot}5088T^4 + 3{\cdot}8466T^2 - 4{\cdot}5135 = 0.$$

j_1	2	3	4	5	6	7
T^2	1·0324	1·0342	1·0436	1·0460	1·0460	1·0460

TABLE 2. Approximations to the time of separation for the boundary-layer case ($k = 0$)

This gives $T^2 = 1{\cdot}032$ compared with $T^2 = 1{\cdot}038$ calculated by the approximation of Blasius (1908). Further approximations corresponding to values of j_1 from 3 to 7 have been calculated by the present method and these are shown in table 2.

The variation of T^2 with R can be investigated by finding the appropriate root of (45) with $i_1 \neq 0$. Calculated results for Reynolds numbers down to $R = 300$ are shown in figure 1, where T^2 is plotted against $1/\log_{10} R$. In these results all the computed terms $G_n^{(i,j)}(x)$ up to $j = 7$ when $i = 0, j = 6$ when $i = 1, j = 5$ when $i = 2$ and $j = 4$ when $i = 3$ were used. The values of n associated with each value of j have already been given. The range of R for which these results are valid is not known but some evidence is available from the results of the fully numerical calculations which are given in the same diagram.

A dimensionless drag coefficient C_D is defined by $C_D = D/\rho a^2 b$, where D is the total drag on the cylinder. It may be expressed as

$$C_D = \frac{4}{R}\int_0^{\pi}\left[\zeta - \frac{\partial\zeta}{\partial\xi}\right]_{\xi=0}\sin\theta\, d\theta, \tag{46}$$

in which the first term in the integral gives the friction drag coefficient C_f and the second the pressure drag coefficient, where $C_D = C_f + C_p$. Both of these coefficients can be calculated as series in powers of τ and k from the present results. It is found, as far as the terms calculated, that

$$\begin{aligned} C_f = \pi(\tau/2R)^{\frac{1}{2}}\{&4{\cdot}5135 + k - 0{\cdot}094k^2 + 0{\cdot}031k^3 + (0{\cdot}0036 + 0{\cdot}238k \\ &- 0{\cdot}938k^2 + 2{\cdot}705k^3)\tau^4 - (0{\cdot}0045 - 0{\cdot}053k + 0{\cdot}459k^2 - 2{\cdot}203k^3)\tau^8 \\ &+ (0{\cdot}00029 + 0{\cdot}00065k)\tau^{12} + O(\tau^{16})\}, \end{aligned} \tag{47}$$

$$\begin{aligned} C_p = \tfrac{1}{4}\pi\{&8{\cdot}0 + 4{\cdot}5135k + k^2 - 0{\cdot}094k^3 + (1{\cdot}256k - 4{\cdot}777k^2 + 13{\cdot}884k^3)\tau^4 \\ &+ (0{\cdot}148k - 2{\cdot}110k^2 + 11{\cdot}307k^3)\tau^8 + 0{\cdot}0133k\tau^{12} + O(\tau^{16})\}. \end{aligned} \tag{48}$$

It may be seen that the drag coefficient is initially constant and equal to 2π, in agreement with boundary-layer theory.

The variation of $R^{\frac{1}{2}}C_f$ with τ is shown for the boundary-layer case ($k = 0$) in figure 2. In figure 3 the variation of $R^{-\frac{1}{2}}\zeta$ with τ is shown over the whole cylinder surface for the boundary-layer solution. The results exhibited in figures 2 and 3 are for the range of values of τ for which they compare satisfactorily with results derived from the numerical procedure described in the last section. Further properties of the flow can be obtained from a knowledge of the vorticity and its derivative with respect to x at the surface of the cylinder. Numerical values of $G_n^{(i,j)}(x)$ and its derivative with respect to x at $x = 0$ are given in tables 3 and 4.

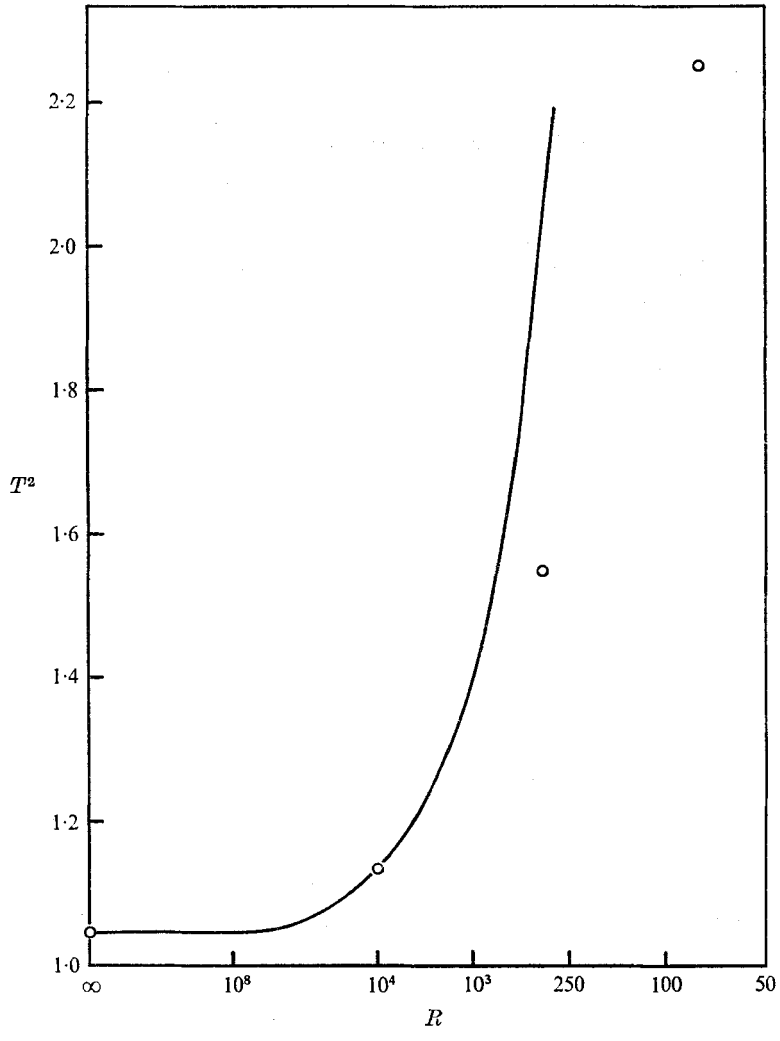

FIGURE 1. Variation of the separation time T with $1/\log_{10} R$. ——, series solution in powers of τ; ○, numerical method.

The fully numerical method of solution was carried out for

$$R^2 = 97{\cdot}5, 5850, 122 \times 10^3 \quad \text{and} \quad \infty.$$

In each case a time $\tau = \tau_M$ (given in table 1) was reached at which the implicit method of integration failed to converge. The value of τ_M decreased with increasing R. The same phenomenon was noted by Collins & Dennis (1973*b*) for the case of the impulsive start. As in that case, the breakdown could possibly be associated with some type of instability in the flow. It is possible that τ_M could be increased by the use of improved iterative methods such as those suggested by Israeli (1970, 1972) but this has not been considered. The three finite Reynolds numbers considered correspond to the three cases $\alpha = 2R^2 = 195, 11700$ and 244×10^3 for which experimental results have been described by Taneda

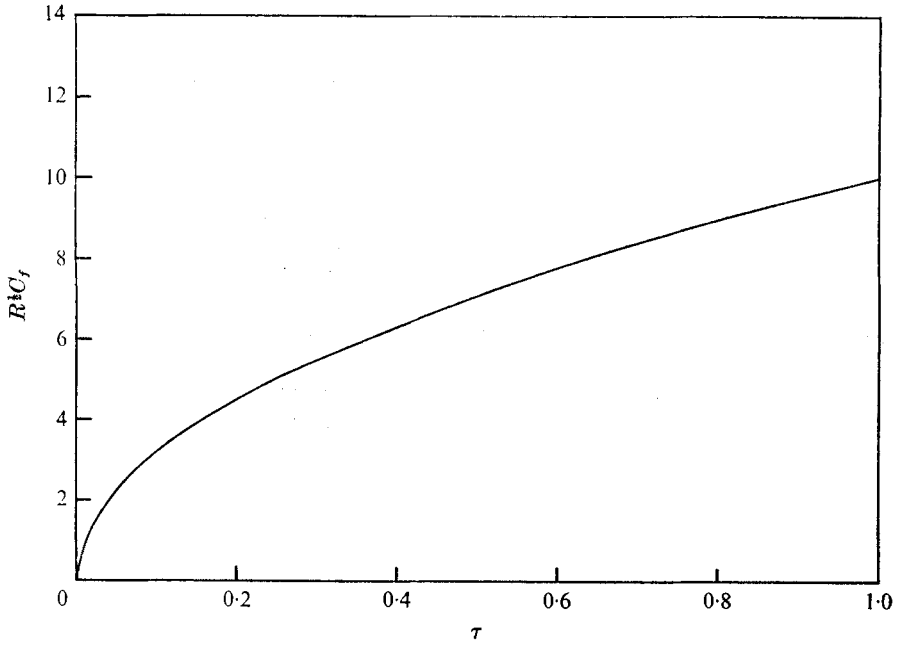

FIGURE 2. Variation of $R^{\frac{1}{2}}C_f$ with τ for the boundary-layer solution obtained from the series in powers of τ.

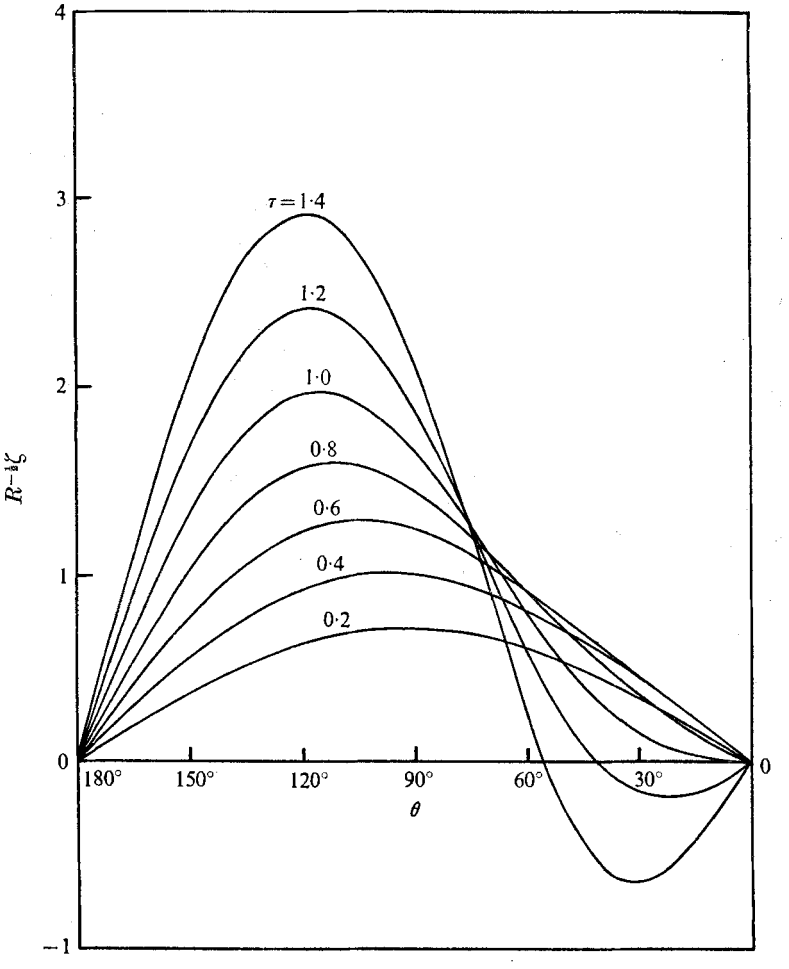

FIGURE 3. Variation of $R^{-\frac{1}{2}}\zeta$ over the surface of the cylinder for the boundary-layer solution obtained from the series in powers of τ.

$x = 0$	$i = 0$	$i = 1$	$i = 2$	$i = 3$
$G_1^{(i,0)}$	4·5135	1·0000	−0·0940	0·0312
$G_2^{(i,1)}$	−1·9233	3·1191	−5·7084	11·178
$G_1^{(i,2)}$	0·0036	0·2380	−0·9385	2·7050
$G_3^{(i,2)}$	−0·1708	1·4940	−7·4925	30·396
$G_2^{(i,3)}$	0·0165	0·2431	−2·4438	14·048
$G_4^{(i,3)}$	−0·0063	0·3843	−4·4246	32·91
$G_1^{(i,4)}$	−0·0045	0·0533	−0·4592	2·2028
$G_3^{(i,4)}$	0·0053	0·0574	−1·5428	24·559
$G_5^{(i,4)}$	0·0054	−0·0048	−1·1446	−15·168
$G_2^{(i,5)}$	−0·0017	0·0336	−0·5409	
$G_4^{(i,5)}$	0·0002	−0·0250	0·0071	
$G_6^{(i,5)}$	0·0020	−0·0512	0·1994	
$G_1^{(i,6)}$	0·0003	0·0006		
$G_3^{(i,6)}$	−0·0001	0·0069		
$G_5^{(i,6)}$	−0·0005	−0·0257		
$G_7^{(i,6)}$	0·0003	−0·0215		
$G_2^{(i,7)}$	0·0002			
$G_4^{(i,7)}$	0·0002			
$G_6^{(i,7)}$	−0·0001			
$G_8^{(i,7)}$	0·0000			

TABLE 3. Numerical values of $G_n^{(i,j)}(0)$

$x = 0$	$i = 0$	$i = 1$	$i = 2$	$i = 3$
$dG_1^{(i,0)}/dx$	−8·0000	−4·5135	−1·000	0·0940
$dG_2^{(i,1)}/dx$	8·0000	−10·526	21·451	−44·894
$dG_1^{(i,2)}/dx$	0	−1·2556	4·7769	−13·884
$dG_3^{(i,2)}/dx$	0	−5·2467	32·742	−144·99
$dG_2^{(i,3)}/dx$	0	−1·7027	14·884	−84·335
$dG_4^{(i,3)}/dx$	0	−1·6483	22·119	−177·588
$dG_1^{(i,4)}/dx$	0	−0·1477	2·1098	−11·307
$dG_3^{(i,4)}/dx$	0	−0·5396	10·565	−121·05
$dG_5^{(i,4)}/dx$	0	−0·1025	6·8908	103·8
$dG_2^{(i,5)}/dx$	0	−0·1188	3·0632	
$dG_4^{(i,5)}/dx$	0	0·1284	0·3797	
$dG_6^{(i,5)}/dx$	0	0·1941	−0·5614	
$dG_1^{(i,6)}/dx$	0	−0·0133		
$dG_3^{(i,6)}/dx$	0	−0·0252		
$dG_5^{(i,6)}/dx$	0	0·2014		
$dG_7^{(i,6)}/dx$	0	0·1040		
$dG_2^{(i,7)}/dx$	0			
$dG_4^{(i,7)}/dx$	0			
$dG_6^{(i,7)}/dx$	0			
$dG_8^{(i,7)}/dx$	0			

TABLE 4. Numerical values of $[dG_n^{(i,j)}/dx]_{x=0}$

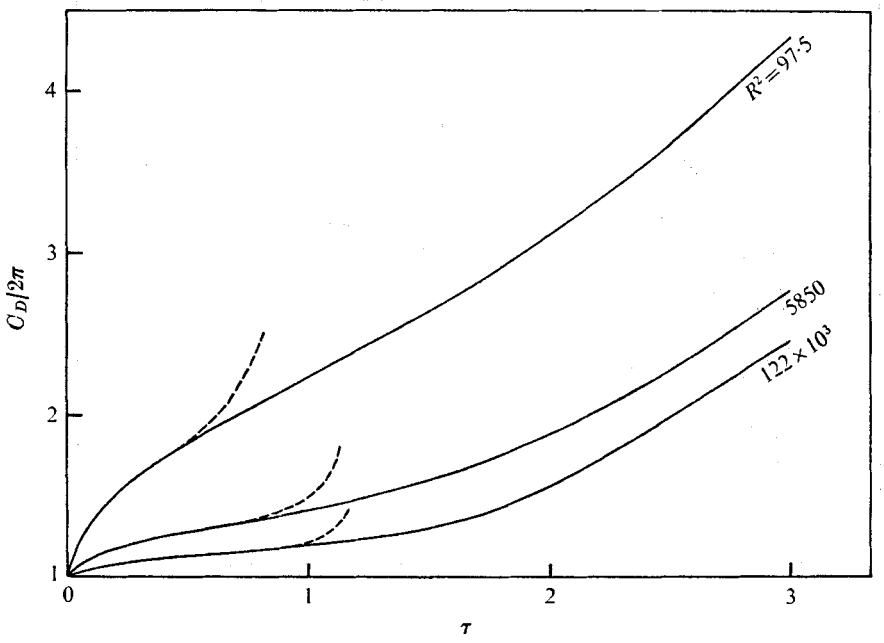

FIGURE 4. Variation of the drag coefficient C_D with τ.
——, numerical method; – – –, series.

(1972). Numerical data relating to these experiments have recently been published by Honji & Taneda (1972) and the comparisons of the present paper are based on the latter. The main property measured was the development with time of the twin pair of vortices formed at the rear of the cylinder.

The frictional and pressure drag coefficients defined in (46) are found to be given by the formulae

$$C_f = 2\pi R^{-1} g_1(0,\tau) = \pi(\tau/2R)^{\frac{1}{2}} G_1(0,\tau), \tag{49}$$

$$C_p = -2\pi R^{-1}[\partial g_1/\partial\xi]_{\xi=0} = -\tfrac{1}{4}\pi[\partial G_1/\partial x]_{x=0}. \tag{50}$$

These quantities have been calculated from the numerical solution, and in figure 4 the variation with τ of the total drag coefficient $C_D = C_f + C_p$ is given. Results calculated from the series (47) and (48) are also shown. The diminishing usefulness of the series method as R decreases is clearly seen, but nevertheless the corrections to boundary-layer theory given by the method are of some value. The variation of the angle of separation θ_s with τ is shown in figure 5 for the Reynolds numbers considered. Calculated values of the time of separation T are given in table 5. An extra value was calculated (corresponding to $R = 10^4$) to help to define the range of validity of the curve in figure 1.

Comparisons of the growth of the length of the vortex pair obtained from the numerical solutions with the data of Honji & Taneda (1972) are given for the three finite Reynolds numbers in figures 6 (*a*)–(*c*). Here $L(\tau)$ is the dimensionless length of the separated region measured in radii along the downstream axis of symmetry from the rearmost point of the cylinder. The Reynolds number range covers the whole range of the data given by Honji & Taneda (1972) and the

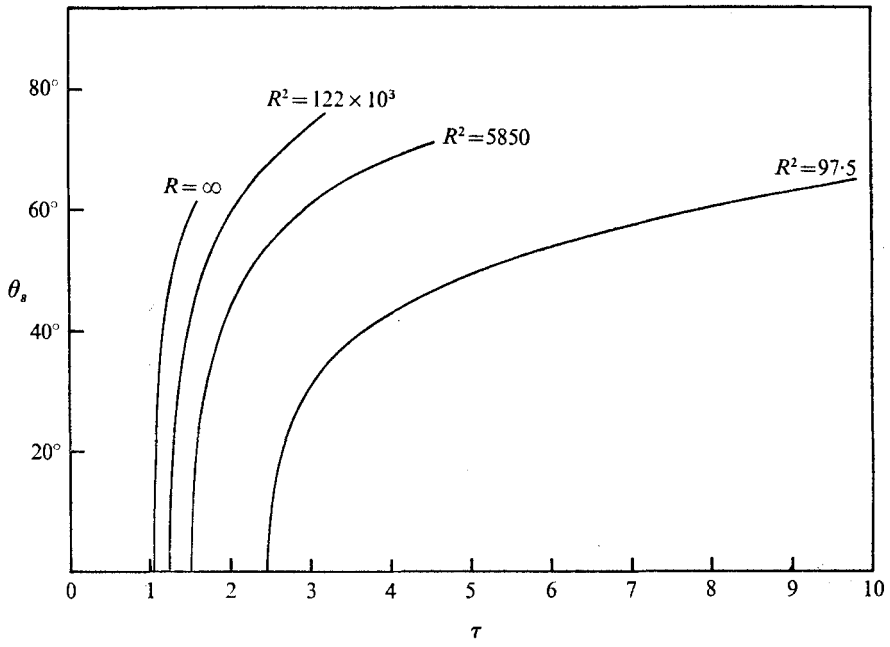

FIGURE 5. Variation of the angle of separation θ_s with τ.

R^2	97·5	5850	122×10^3	10^8	∞
Numerical solution	2·460	1·501	1·245	1·065	1·023
Series solution	—	—	1·421	1·068	1·023

TABLE 5. Calculated values of the time of separation T

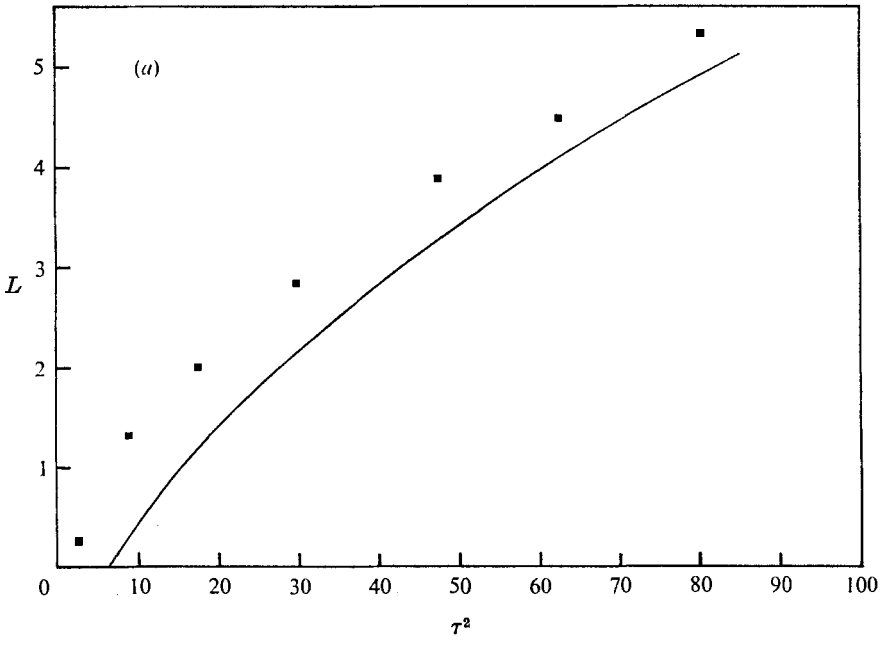

FIGURE 6(a). For legend see facing page.

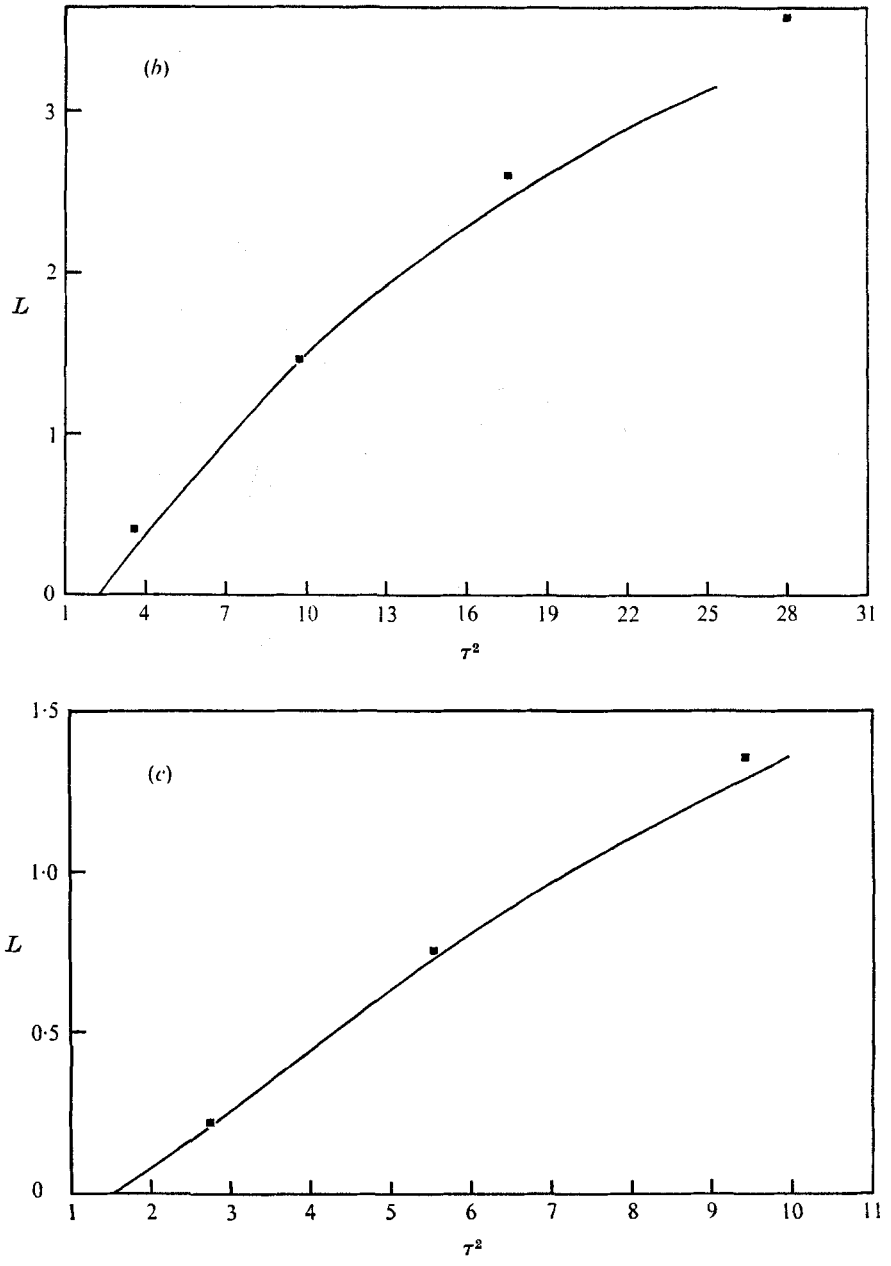

FIGURE 6. Variation of the wake length L as a function of τ^2 for (*a*) $R^2 = 97{\cdot}5$, (*b*) $R^2 = 5850$, (*c*) $R^2 = 122 \times 10^3$. Numerical solution: ——, present study. Experimental measurements: ■, Honji & Taneda (1972).

degree of agreement is variable, being barely satisfactory at $R^2 = 97{\cdot}5$ to good at $R^2 = 122 \times 10^3$. It is difficult to identify the cause of the discrepancy at $R^2 = 97{\cdot}5$, but there is no obvious reason why the present results should be less accurate at lower Reynolds numbers. The main source of the discrepancy appears to lie in a much earlier separation of the flow in the experimental study

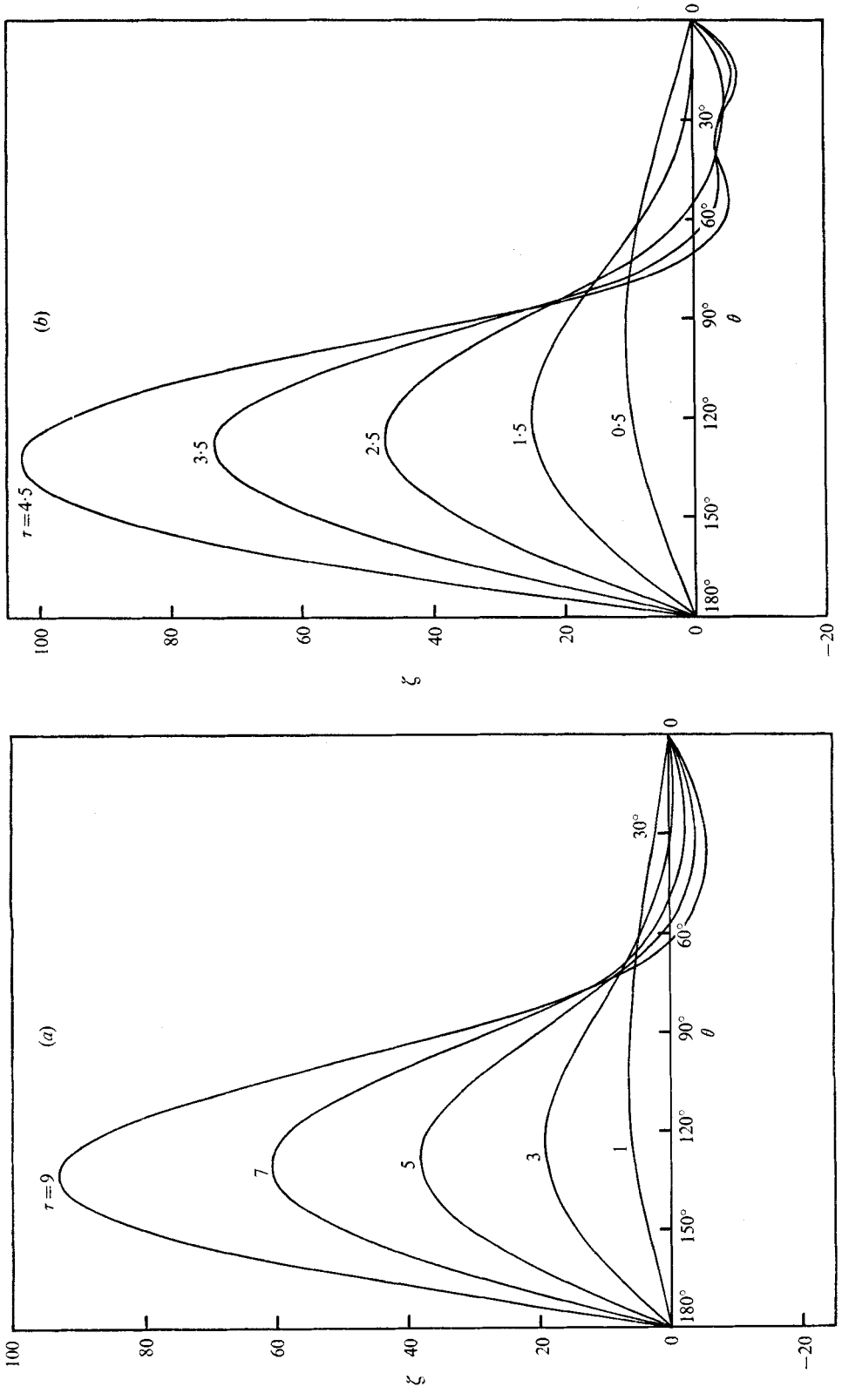

FIGURES 7 (*a*), (*b*). For legend see facing page.

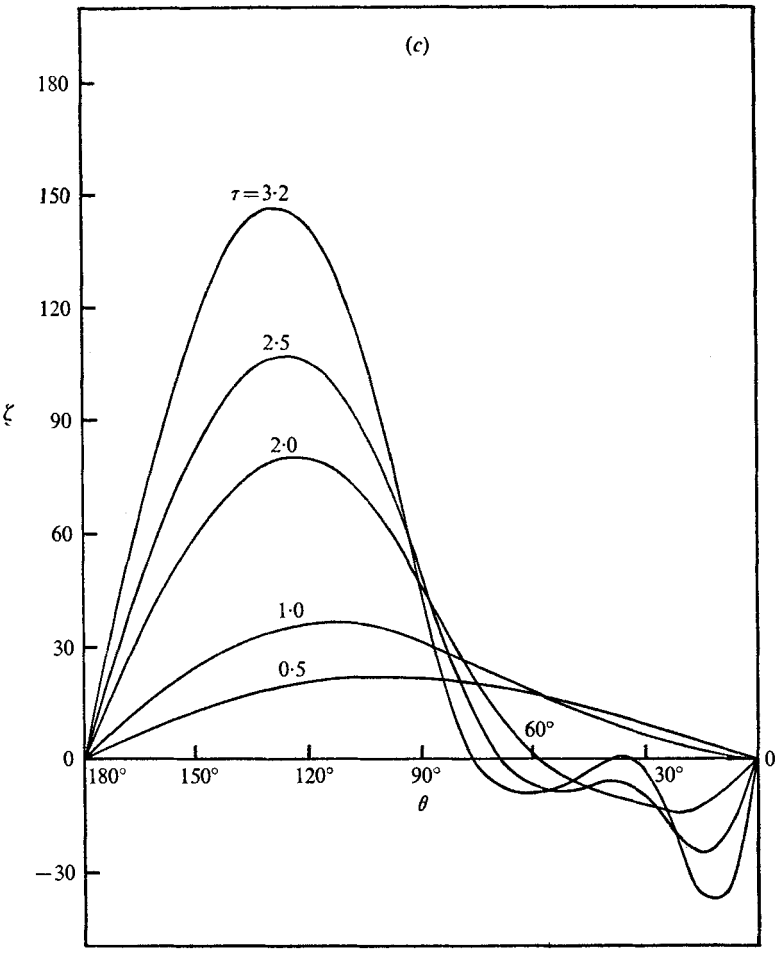

FIGURE 7. Variation of ζ over the surface of the cylinder for (*a*) $R^2 = 97{\cdot}5$, (*b*) $R^2 = 5850$, (*c*) $R^2 = 122 \times 10^3$.

than in the calculations. The value of T obtained for $R^2 = 97{\cdot}5$ in the calculations cannot be checked by the power-series method, but since only a few terms of the series (7) and (8) are significant when separation occurs, the estimate of T is thought to be accurate.

The development with τ of the dimensionless vorticity ζ over the surface of the cylinder is shown for the cases $R^2 = 97{\cdot}5, 5850$ and 122×10^3 in figures 7 (*a*)–(*c*). For the lowest value of R the variation of ζ in the region of separated flow exhibits a single local minimum for the entire range of τ. This is also true in the case $R^2 = 5850$ for small τ, but at about $\tau = 3{\cdot}5$ a local maximum develops in the region of separated flow $0 < \theta < \theta_s$ and the vorticity in this region remains distorted until the final time $\tau_M = 4{\cdot}7$. A similar situation occurs in the solution for $R^2 = 122 \times 10^3$, but in this case the local maximum in the separated region starts to occur at an earlier value of τ and develops to such an extent that a secondary vortex appears in the region $0 < \theta < \theta_s$ at about $\tau = 3$. The integration terminated soon after (at $\tau_M = 3{\cdot}2$) because of its failure to converge. Taneda

(1972) has stated that secondary vortices were observed to occur experimentally for $R^2 > 25 \times 10^4$ at a value of τ equal to about 4.

Finally, for the boundary-layer case ($R = \infty$) the integration could not be continued beyond $\tau = 1{\cdot}6$. For values of τ up to $\tau = 1{\cdot}4$ the results of the numerical integration were found to be in good agreement with the results obtained from the series in powers of τ. For example, the numerical solution gives results for the variation of $R^{-\frac{1}{2}}\zeta$ over the cylinder surface which are in complete agreement with the results of figure 3. Other properties show a similar good agreement.

This work was supported by grants from the National Research Council of Canada.

REFERENCES

Blasius, H. 1908 *Z. angew. Math. Phys.* **56**, 1.

Collins, W. M. & Dennis, S. C. R. 1973*a* *Quart. J. Mech. Appl. Math.* **26**, 53.

Collins, W. M. & Dennis, S. C. R. 1973*b* *J. Fluid Mech.* **60**, 105.

Goldstein, S. & Rosenhead, L. 1936 *Proc. Camb. Phil. Soc.* **32**, 392.

Görtler, H. 1944 *Ing.-Arch.* **14**, 286.

Görtler, H. 1948 *Arch. Math. Karlsruhe*, **1**, 138.

Honji, H. & Taneda, S. 1972 *Rep. Res. Inst. Appl. Mech., Kyushu University*, **19**, 265.

Israeli, M. 1970 *Studies in Appl. Math.* **49**, 327.

Israeli, M. 1972 *Studies in Appl. Math.* **51**, 67.

Orszag, S. A. 1970 *J. Atmos. Sci.* **27**, 890.

Orszag, S. A. 1971 *Studies in Appl. Math.* **50**, 293.

Taneda, S. 1972 *Recent Research on Unsteady Bounday Layers*, vol. 2 (ed E. A. Eichelbrenner), pp. 1165–1215. Quebec: Laval University Press.

Wang, C. Y. 1967 *J. Math. Phys.* **46**, 195.

Watson, E. J. 1955 *Proc. Roy. Soc.* A **231**, 104.